Cell Biol Toxicol (2024) 40:102
https://doi.org/10.1007/s10565-024-09925-x

RESEARCH

ASPP2 deficiency attenuates lipid accumulation through the PPARγ pathway in alcoholic liver injury

Ying Zhang · Xingzhong Miao · Fang Liu · Honglin Shi · Dexi Chen · Yu Chen · Yingmin Ma · Hongbo Shi

Received: 16 May 2024 / Accepted: 2 October 2024 / Published online: 22 November 2024

Abstract The initial stage of alcoholic liver disease (ALD) is hepatic steatosis. Recent studies have highlighted a possible role for Apoptosis-stimulating protein 2 of p53 (ASPP2) in regulating hepatic lipid metabolism in nonalcoholic fatty liver (NAFLD). However, whether ASPP2 regulates alcohol-induced lipid accumulation and its mechanisms remain unclear. To explore that, we establish an alcoholic liver injury model in vivo and in vitro. The clinical specimens were collected from liver tissues of patients with alcoholic liver disease. Lipid metabolism was detected by HE staining, oil red O staining and qPCR; and ASPP2-peroxisome proliferator-activated receptor γ (PPARγ) signaling pathways were detected by western blot and immunohistochemical staining. We found that both ASPP2 and PPARγ expression increased in patients and mouse models with ALD. We also discovered the reduction of ASPP2 significantly inhibited the expression of PPARγ and alleviated alcohol-induced hepatic lipid accumulation and liver injury in vivo and in vitro. Mechanistically, the PPARγ agonist reversed the protective effect of ASPP2 downregulation on hepatic steatosis and liver injury, while the opposite results were observed using PPARγ inhibitor. In conclusion, ASPP2 exacerbates ethanol-induced lipid accumulation and hepatic injury by upregulating the PPARγ signaling pathway, thus promoting the occurrence and development of ALD.

Keywords Alcoholic liver disease · ASPP2 · PPARγ · Hepatic steatosis · Lipid metabolism

Abbreviations

ALD	Alcoholic liver disease
NAFLD	Nonalcoholic fatty liver
PPARγ	Peroxisome proliferator-activated receptor
ASPP2	Apoptosis-stimulating protein 2 of p53
mTORC1	Mammalian target of rapamycin complex 1
ApoB	Apolipoprotein B
MTTP	Microsomal triglyceride transfer protein
LFABP	Liver Fatty acid binding protein
CD36	CD36 molecule, fatty acid translocase
CPT1A	Carnitine Palmitoyltransferase 1A
AOX	Acyl-CoA oxidase 1
ACC1	Acetyl Coenzyme A Carboxylase 1

Supplementary Information The online version contains supplementary material available at https://doi.org/10.1007/s10565-024-09925-x.

Y. Zhang · X. Miao · Y. Chen · H. Shi (✉)
Beijing Municipal Key Laboratory of Liver Failure and Artificial Liver Treatment Research, Fourth Department of Liver Disease, Beijing Youan Hospital, Capital Medical University, Beijing, China
e-mail: shihongbo@ccmu.edu.cn

F. Liu · H. Shi · D. Chen · Y. Ma (✉)
Beijing Institute of Hepatology, Beijing Youan Hospital, Capital Medical University, Beijing, China
e-mail: mayingmin@ccmu.edu.cn

FAS	Fatty acid synthase
ALT	Alanine aminotransferase
AST	Aspartate Transaminase
TC	Serum total cholesterol
TG	Triglyceride

Background

Alcohol abuse causes a series of liver injuries, collectively known as alcoholic liver disease (ALD) (Sehrawat et al. 2020). Alcohol-related deaths account for 6% of global mortality (Bajaj 2019). And alcohol abuse is a major risk factor for premature death and disability among individuals aged 15–49 (Xu et al. 2018). Alcohol abuse causes a world public health problem, but there is no specific drug for treatment of ALD except abstinence from alcohol. ALD includes various histopathologic changes, ranging from simple steatosis to alcoholic steatohepatitis, progressive liver fibrosis, cirrhosis, and liver cancer (Singal et al. 2018). Studies have shown that simple steatosis can be reversed by ceasing alcohol intake (Fuster and Samet 2018). Hence, it is crucial to intervene simple steatosis early to prevent from progressing to the steatohepatitis in ALD.

Apoptosis-stimulating protein 2 of p53 (ASPP2) is a member of the p53 binding protein family, playing a pro-apoptotic role by binding to p53 protein (Tian et al. 2018). In addition, ASPP2 has been shown to inhibit autophagy, maintain energy balances and exert an inhibitory effect on tumors [(Turnquist et al. 2014); (Song et al. 2015)].

A recent study showed that ASPP2 can regulate the mammalian target of rapamycin complex 1 (mTORC1) signaling pathway (Yao et al. 2022). And research has shown that mTORC1 plays an important role in lipid metabolism (Ouyang and Liu 2022). One research suggested that ASPP2 may reduce the level of triglycerides by inhibiting autophagy in nonalcoholic fatty liver (NAFLD), but its regulatory mechanism for lipid metabolism was not specifically elucidated (Xie et al. 2015). However, the role of ASPP2 in alcoholic induced lipid accumulation has been poorly studied. Therefore, in the present study, we attempted to investigate the role of ASPP2 in the regulation of lipid metabolism in ALD and provide a new therapeutic target for treating ALD.

Methods

Antibodies and reagents

ASPP2 adenovirus (adv-ASPP2), ASPP2-siRNA, and ASPP2 short hairpin RNA lentivirus (LV-ASPP2 shRNA) were purchased from Hesheng Gene Technology Co., Ltd. (Beijing, China). The PPARγ agonist rosiglitazone (R2408) was purchased from Sigma; the PPARγ inhibitor T0070907 (HY-13202) was purchased from MedChemExpress (MCE). Antibodies against β-actin, phospho-mTOR (Ser2448), phospho-S6 ribosomal protein (Ser235/236), and phospho-p70 S6 kinase (Thr389) were purchased from Cell Signaling Technology; anti-ASPP2 antibody for western blotting was from Sigma; anti-ASPP2 antibody used for immunohistochemical staining was from Abcam; and anti-PPARγ antibody was from Abcam. Alexa Fluor® 594-conjugated goat anti-rabbit IgG (H + L) (Affinity Purified) was purchased from Beijing Zhongshan Jinqiao Biotechnology Co. Ltd. Peroxidase-conjugated secondary antibodies were from Sigma.

Animal experiments

ASPP2-knockdown (ASPP2-KD) mice and controls (8–10 weeks old, body weight 20–25 g, male) were provided by the Animal Center of Beijing Institute of Hepatology, China. The Lieber-DeCarli ethanol diet (TP4030D) and the isocaloric control liquid diet (TP4030C) were purchased from Jiangsu Nantong Trophic Animal Feed High-Tech Co., Ltd., China.

The study was approved by the Animal Experiments and Experimental Animal Welfare Committee of Capital Medical University (AEEI-2022–117), China. All animal procedures were performed following the "Guide for the Care and Use of Laboratory Animals" published by the National Institutes of Health. According to the National Institute on Alcohol Abuse and Alcoholism (NIAAA) models, control and ASPP2-KD mice were fed ad libitum the Lieber-DeCarli diet containing 5% ethanol (v/v) for 4 weeks plus a single binge feeding by oral gavaging. Nine hours after binge feeding, animals were employed in various experimentations (Bertola et al. 2013). For rosiglitazone, we gave the rosiglitazone (5 mg/kg/Day) to wild-type mice and ASPP2-KD mice that received the ethanol diet.

Cell culture

HL-7702 cell lines were obtained from Beijing Institute of Hepatology, China. Primary hepatocytes were isolated from C57/BJ mice. For the overexpression of HL-7702 and primary hepatocyte, HL-7702 cells and primary hepatocytes were transfected with adenovirus (Adv) -GFP-ASPP2 (Ad-ASPP2) and Adv-GFP (as the control) for 24 h and then treated with 200 mM ethanol for 12 h, 24 h, and 48 h, respectively. The HL-7702 cells and primary hepatocyte transfected with adv-ASPP2 and adv-GFP were pretreated with T0070907 for 2 h followed by induction with alcohol for 24 h. The HL-7702 cell model with low expression of ASPP2 were prepared by lentivirus (LV) -ASPP2 shRNA and LV-control and then treated with ethanol for 12 h, 24 h, and 48 h, respectively. Primary hepatocytes with low expression of ASPP2 were constructed with ASPP2-siRNA. The HL-7702 cells and primary hepatocytes with low expression of ASPP2 were pretreated with 20 mM rosiglitazone/T0070907 for 2 h and then induced with alcohol for 24 h.

Patients

Liver tissues from patients with ALD and normal liver tissues were obtained from liver transplantation at Beijing You'an Hospital, Capital Medical University. A total of 3 samples of alcoholic cirrhosis patients were collected. All 3 patients were male, aged 38,58,52 years old, and all had a long history of alcohol consumption. And the normal liver specimen was derived from liver tissue discarded during liver transplant surgery when necessary repairs are made to the donor liver. The diagnosis of ALD was based on the Guidelines of Prevention and Treatment for Alcoholic Liver Disease (2018 update). The study was approved by the Ethics Committee of Beijing You'an Hospital, Capital Medical University, China (Jingyoukelun2022037). And the informed consent of patients was obtained for this study.

Table 1 Real-time PCR Primer Sequences for Human

Gene	Forward (5'-3')	Reverse (5'-3')
β-actin	CTCACCATGGATGATGATATCGC	AGGAATCCTTCTGACCCATGC
ApoB	ACACACTGGACGCTAAGAGGA	ACTTGTGCTACCATCCCATACT
MTTP	ACAAGCTCACGTACTCCACTG	TCCTCCATAGTAAGGCCACATC
LFABP	GTGTCGGAAATCGTGCAGAAT	GACTTTCTCCCCTGTCATTGTC
CPT1A	ATGCGCTACTCCCTGAAAGTG	GTGGCACGACTCATCTTGC
AOX	ATGCCTGTCTGATTCCCATCT	CATGACACTTGGCAATCCTCT
CD36	AAGCCAGGTATTGCAGTTCTTT	GCATTTGCTGATGTCTAGCACA
ACC1	ATGTCTGGCTTGCACCTAGTA	CCCCAAAGCGAGTAACAAATTCT
FAS	GCATCTGGACCCTCCTACCT	ACCTGGAGGACAGGGCTTAT
PPARγ	GCCGAGAAGGAGAAGCTGTT	CTCGCCTTTGCTTTGGTCAG

Table 2 Real-time PCR Primer Sequences for Mouse

Gene	Forward (5'-3')	Reverse (5'-3')
β-actin	CTGTCCCTGTATGCCTCTG	ATGTCACGCACGATTTCC
ApoB	TCACCATTTGCCCTCAACCTAA	GAAGGCTCTTTGGAAGTGTAAAC
MTTP	AACTCCTACGAGCCCTCCTT	AGTCCTCCCAGGATCAGCTT
LFABP	GCAGAGCCAGGAGAACTTTGAG	TTTGATTTTCTTCCCTTCATGCA
CPT1A	CTCCGCCTGAGCCATGAAG	CACCAGTGATGATGCCATTCT
AOX	CCGACCCAAGAGCTGATATTTC	CCATGTCACCCTCTCACCATAA
CD36	GTGCAAAACCCAGATGACGT	TCCAACAGACAGTGAAGGCT
ACC1	CATGTCATTGTTCCTGGTCAAAC	AAGAGCCTCCTCTTAGCCACCTC
FAS	GCGGGTTCGTGAAACTGATAA	GCAAAATGGGCCTCCTTGATA
PPARγ	GCCAAGGTGCTCCAGAAGAT	GGGTGAAGGCTCATGTCTGT

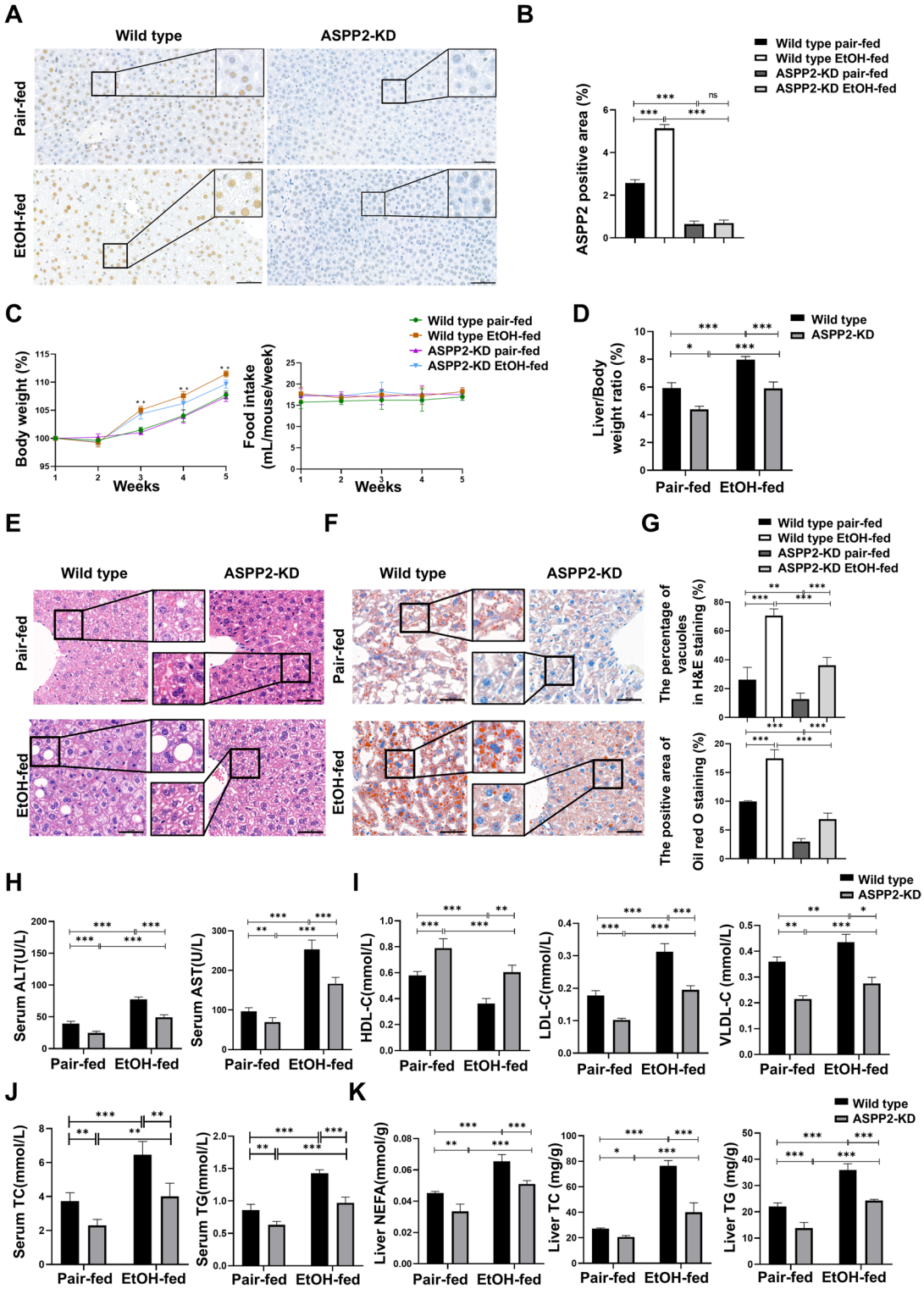
A
Wild type
ASPP2-KD
Pair-fed
EtOH-fed
B
Wild type pair-fed
Wild type EtOH-fed
ASPP2-KD pair-fed
ASPP2-KD EtOH-fed
ASPP2 positive area (%)
C
Body weight (%)
Weeks
Food intake (mL/mouse/week)
D
Wild type
ASPP2-KD
Liver/Body weight ratio (%)
E
F
G
The percentage of vacuoles in H&E staining (%)
The positive area of Oil red O staining (%)
H
Serum ALT(U/L)
Serum AST(U/L)
I
HDL-C(mmol/L)
LDL-C(mmol/L)
VLDL-C (mmol/L)
J
Serum TC(mmol/L)
Serum TG(mmol/L)
K
Liver NEFA(mmol/g)
Liver TC (mg/g)
Liver TG (mg/g)

◂**Fig. 1** Reduction of hepatic ASPP2 alleviates ethanol-induced hepatic steatosis and injury in a mouse model. ASPP2-KD mice and wild-type mice were fed the Lieber-DeCarli liquid alcohol diet or the control liquid diet for four weeks plus 1 binge. (**A** and **B**) Representative IHC analysis of ASPP2 in liver sections, scar bar = 50 μm (**A**) and quantification analyses (**B**) of ASPP2 positive area (%). The extended part of the black lines shows the enlarged image from the black box area. (**C**) Changes in body weight (left) and food intake (right). $*P < 0.05$, wild-type pair-fed vs. wild-type EtOH-fed; $+P < 0.05$, ASPP2-KD pair-fed vs. ASPP2-KD EtOH-fed. (**D**) Liver/Body weight ratios. (**E** and **F**) Representative H&E staining (**E**) and representative oil red O staining (**F**) of liver tissue, scar bar = 50 μm. (**G**) Analyses of the percentage of vacuoles in H&E staining (top) and the positive area in oil red O staining (bottom). (**H**) Serum ALT and AST levels. (**I**) Serum HDL, LDL and VLDL levels. (**J**) Serum TC and TG levels. (**K**) Liver NEFA, TC and TG levels. The values represent the means ± SEMs ($n = 6$ in each group). nsP > 0.05, $*P < 0.05$, $**P < 0.01$, $***P < 0.001$. Independent-samples T tests between two groups and one-way ANOVA followed by Bonferroni post hoc test for multiple comparisons were used for statistical analyses

Histopathology and immunohistochemical staining

The paraffin-embedded liver tissue blocks were cut into 5 mm-thick sections and then stained with hematoxylin and eosin (H&E), and the frozen liver tissues were cut into 8 mm-thick sections and then stained with oil red O. For immunohistochemistry, paraffin sections were deparaffinized with xylene solution after baking in an oven at 67 °C for two hours, followed by dehydration with alcohol. After dehydration, the antigen was repaired by microwave treatment at 100 °C for 10 min in a citrate solution with pH 6.0. Then, the deparaffinized samples were added to a 3% H_2O_2 solution and incubated at room temperature for 15 min to block the inactivation of endogenous peroxidase. Subsequently, the sections were blocked with 5% goat serum at room temperature for 1 h and then incubated with primary anti-ASPP2 or anti-PPAR gamma antibody at 4 °C overnight, followed by secondary antibody conjugated to horseradish peroxidase (HRP) (Cell Signaling, CA, USA) at 37 °C for 30 min. Finally, the expression of ASPP2 or PPARγ was observed by microscopy (Leica Microsystems, Mannheim, Germany) after development using a diaminobenzidine kit (Boster, Wuhan, China). And the Image J is used for quantitative analysis. First, set the scale with a line as long as the ruler in the Image J software, then circle the cell outline to measure the area. Then the small vacuoles in the cells were circled, all of the vacuole area in the cell was accumulated, and the ratio of the two was calculated. Finally, select 8–10 cells to calculate the average.

Western blot analysis

Protein extracts from cell and liver tissues were generated with RIPA buffer supplemented with 1 mM phenylmethylsulfonyl fluoride (PMSF). Protein extracts were separated by SDS−PAGE and transferred to polyvinylidene difluoride (PVDF) membranes. The membranes were incubated with appropriate primary antibodies at 4 °C overnight. Then, HRP-conjugated secondary antibodies were applied at room temperature for 1 h. Finally, the immune complexes were detected using ECL detection reagents (Millipore, USA). Image J software was used for the quantification of band densitometries.

Quantitative real-time PCR analysis

Total RNA was extracted using TRIzol reagent (Invitrogen, USA) and then transcribed into cDNA using PrimeScript™ 1st Strand cDNA Synthesis Kit (Takara, China) according to the manufacturer's instructions. Real-time PCR was performed with an Applied Biosystems 7300 Real-Time PCR System (Thermo, USA) using TB Green® Premix Ex Taq™ (Takara, China). The mRNA expression was normalized to the expression of the housekeeping gene *β-actin*. All primer sequences presented in Table 1 were from PrimerBank and synthesized by Hesheng Gene Technology Co., Ltd. (Beijing, China) Table 2.

Immunostaining and confocal microscopy

HL-7702 cells were fixed with 4% paraformaldehyde at room temperature for 20 min and then washed with phosphate-buffered saline (PBS). After fixation, the cells were exposed to 0.1% Triton X-100 in PBS for 10 min for permeabilization. Then, the cells were blocked with PBS plus 10% fetal bovine serum at room temperature for 1 h, followed by primary anti-PPAR gamma antibody at 4 °C overnight. Subsequently, Alexa Fluor® 594-conjugated goat anti-rabbit IgG was used at room temperature for 1 h. Finally, coverslips were mounted with an anti-fading

agent. Images were obtained on a Leika SP8 lightning confocal microscope with Airyscan or His-SIM (High Sensitivity Structural Illumination) superresolution imaging.

Biochemical analysis

Serum alanine aminotransferase (ALT), aspartate aminotransferase (AST), cholesterol (TC), triglyceride (TG), high-density lipoprotein-cholesterol (HDL-C), low-density lipoprotein-cholesterol (LDL-C), and very-low-density lipoprotein-cholesterol (VLDL-C) levels were measured by a biochemical analyzer (Cobas-Mira Plus, Roche Manheim, Germany) according to the instructions of commercial assay kits from the manufacturer (Jiancheng Biotech, Nanjing, China).

Statistical analysis

All data are presented as the mean ± SEM. Statistical significance was determined by GraphPad Prism 8 (San Diego, CA, USA). A two-sample unpaired Student's t test was used for two-group comparisons. Two-way ANOVA followed by Tukey's test was used for measurements from multiple groups. The differences were statistically significant: $*p < 0.05$, $**p < 0.01$, and $***p < 0.001$.

Results

Reduction of hepatic ASPP2 alleviates hepatic steatosis and injury in a mouse model of ALD

To explore the possible role of ASPP2 in ALD, we first performed immunohistochemistry analysis to determine whether the expression of ASPP2 in the liver was altered by ethanol consumption. We found that the expression of ASPP2 increased significantly in mice that received the ethanol diet, which was approximately twofold greater than that observed in pair-fed mice, and ASPP2 was mainly expressed in the nucleus of hepatocytes (Fig. 1A, B). We then compared the ethanol-induced body weight change between ASPP2-KD mice and wild-type mice. As shown in Fig. 1C (left), the body weight of the mice that received the ethanol diet and pair-fed diet increased gradually, and compared to that of pair-fed mice, the body weight of the ethanol-fed mice increased more significantly. However, there was no significant difference in weight gain between ethanol-fed wild-type mice and ASPP2-KD littermates. In addition, the decrease of ASPP2 also did not affect food intake in either group mice (Fig. 1C, right). Alcohol increased the liver/body weight ratios of mice, but liver/body weight ratios in ASPP2-KD mice were significantly lower compared to wild-type mice (Fig. 1D). Next, we assessed ethanol-induced hepatic steatosis by H&E staining and oil red O staining. Livers from ethanol-fed ASPP2-KD mice showed a significantly decreased number and size of vacuoles and lipid droplets compared with those from wild-type mice, indicating that lipid accumulation diminished (Fig. 1E–G). Furthermore, ethanol resulted in a significant increase in serum ALT and AST, while reduction of ASPP2 significantly reduced ethanol-induced elevation of ALT and AST levels (Fig. 1H). In addition, compared with wild-type mice, the levels of low-density lipoprotein-cholesterol (LDL-C), and very-low-density lipoprotein-cholesterol (VLDL-C) in ethanol-fed ASPP2-KD mice showed a significant downward trend (Fig. 1I). Accordingly, TC and TG levels in the serum of ethanol-fed ASPP2-KD mice were significantly reduced compared with that of wild-type mice (Fig. 1J). Consistent with this, lower levels of NEFA, TC and TG were also detected in the liver tissues of ASPP2-KD mice (Fig. 1K).

Collectively, these results indicate that decrease of ASPP2 induced a clear protective effect against ethanol-induced hepatic lipid accumulation and liver injury.

ASPP2 deficiency inhibits PPARγ and mTOR signaling in alcoholic liver injury

To elucidate the molecular mechanism underlying the reduced hepatic steatosis in ethanol-fed ASPP2-KD mice, we investigated the activation of PPARγ signaling, a key pathway regulating hepatic lipid metabolism. Firstly, through immunohistochemical analysis, we detected that ethanol resulted in a significant increase in PPARγ expression in wild-type mice, while the expression of PPARγ was significantly decreased in ASPP2-KD mice compared with wild-type mice. Moreover, in addition to the high expression of PPARγ in the nucleus, we found that the expression of PPARγ in the cytoplasm was increased due to ethanol (Fig. 2 A, B). As illustrated in Fig. 2 C and D, compared with pair-fed diet feeding, both wild-type and ASPP2-KD mice, the protein

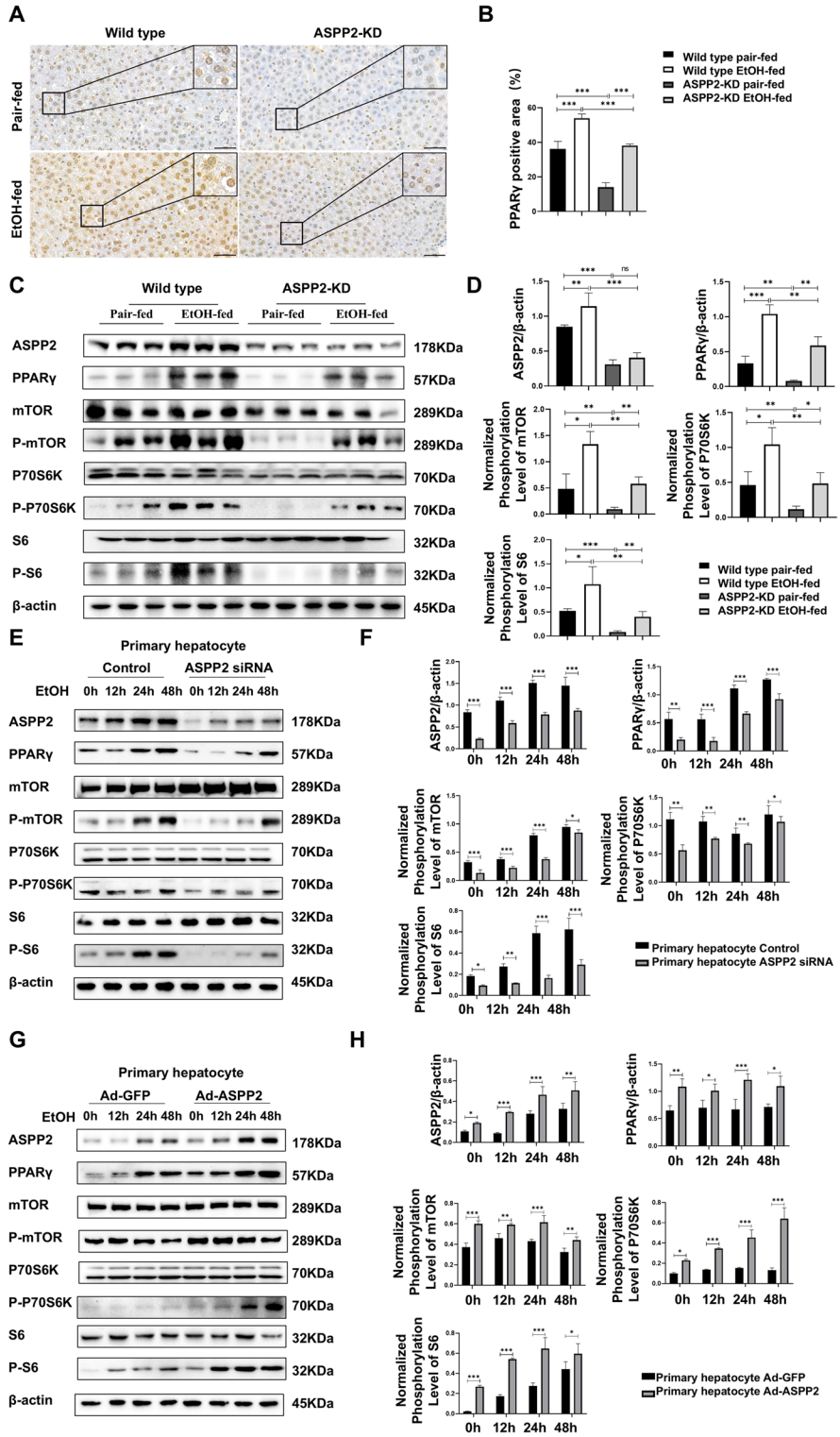

Fig. 2 ASPP2 deficiency inhibits the PPARγ and mTOR signaling pathways. (A and B) Representative IHC analysis of PPARγ in liver sections, scar bar = 50 μm (**A**) and quantification analyses (**B**) of PPARγ positive area (%) in mouse liver tissue from wild-type mice and ASPP2-KD mice. The extended part of the black lines shows the enlarged image from the black box area. (**C** and **D**) western blot (**C**) and quantification analyses (**D**) of ASPP2, PPARγ, phospho-mTOR, phospho-S6, phospho-p70S6K, and β-actin in mouse liver tissue from wild-type mice and ASPP2-KD mice. (**E** and **F**) western blot (**E**) and quantification analyses (**F**) of ASPP2, PPARγ, phospho-mTOR, phospho-S6, phospho-p70S6K, and β-actin in primary hepatocytes (Control and ASPP2 siRNA) treated with ethanol for different times. (**G** and **H**) western blot (**G**) and quantification analyses (**H**) of ASPP2, PPARγ, phospho-mTOR, phospho-S6, phospho-p70S6K, and β-actin in primary hepatocytes (Ad-GFP and Ad-ASPP2) with the indicated treatment. The values represent the means ± SEMs ($n = 6$ in each group). nsP > 0.05, *$P < 0.05$, **$P < 0.01$, ***$P < 0.001$. Independent-samples T tests between two groups were used for statistical analysis, and one-way ANOVA followed by Bonferroni post hoc tests for multiple comparisons were used for statistical analyses

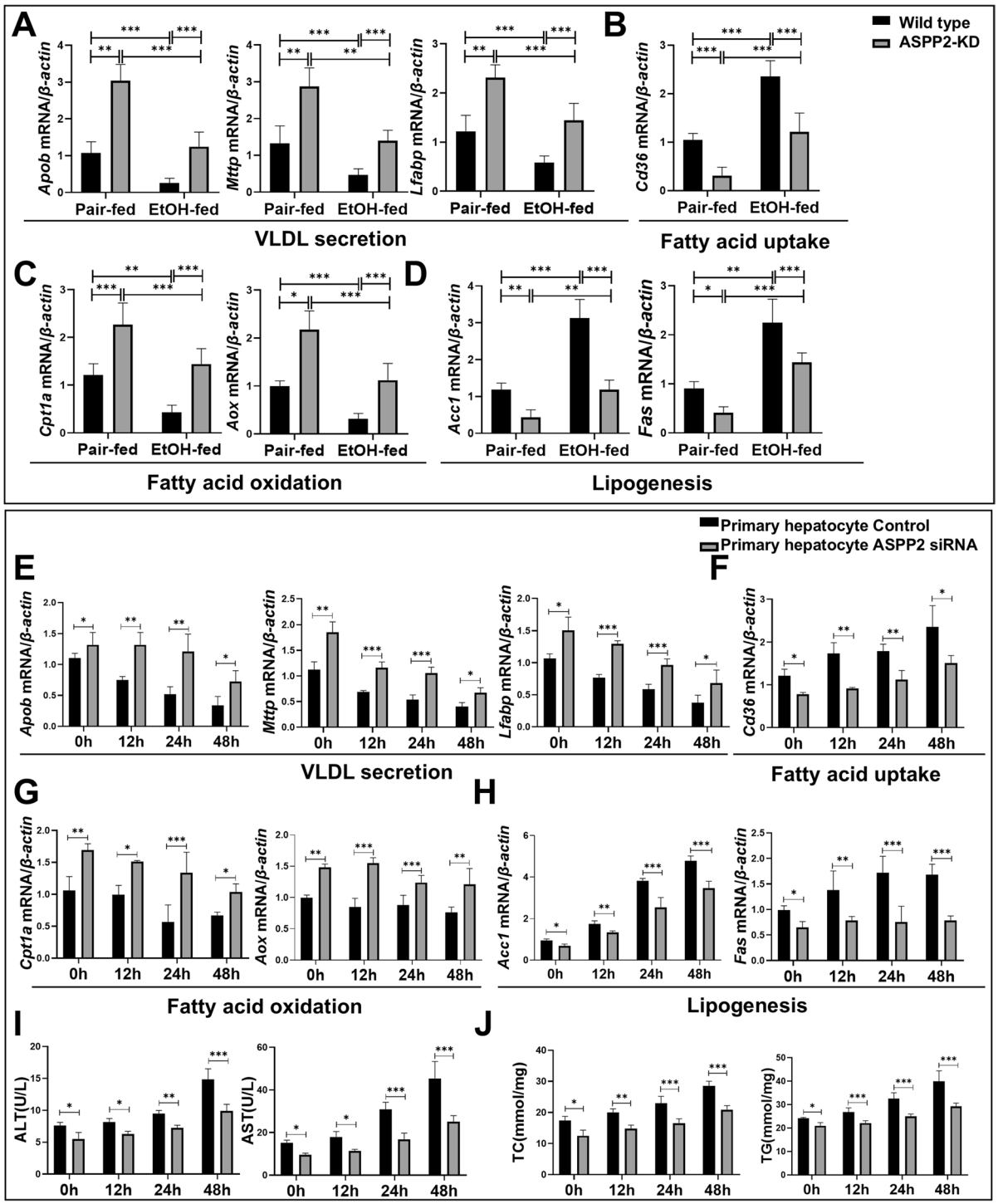

expression of PPARγ and the phosphorylation of mTOR (Ser2448), p70 S6 kinase (Thr389), and S6 ribosomal protein (Ser235/236) were obviously higher in ethanol-fed mice. In addition, the expression levels of these proteins were lower in the liver tissue of ASPP2-KD mice than in wild-type mice.

To further verify the regulatory effect of ASPP2 on PPARγ, we used siRNA and shRNA to prepare primary

◂**Fig. 3** ASPP2 deficiency reduces liver lipid accumulation by promoting fatty acid decomposition and utilization and by inhibiting the synthesis and uptake of fatty acids. (**A**, **B**, **C**, and **D**) The mRNA levels of genes involved in lipid metabolism in mouse liver tissue measured by real-time PCR. (**E**, **F**, **G**, and **H**) The mRNA levels of genes involved in lipid metabolism in ethanol-treated primary hepatocytes (Control and ASPP2 siRNA) measured by real-time PCR. (**I**) ALT and AST levels in the cell supernatant of ethanol-treated primary hepatocytes (Control and ASPP2 siRNA). (**J**) TC and TG levels in the cell supernatant of ethanol-treated primary hepatocytes (Control and ASPP2 siRNA). The values represent the means ± SEMs ($n = 6$ in each group). nsP > 0.05, $^{*}P < 0.05$, $^{**}P < 0.01$, $^{***}P < 0.001$. Independent-samples T tests between two groups were used for statistical analysis, and one-way ANOVA followed by Bonferroni post hoc tests for multiple comparisons were used for statistical analyses

hepatocytes and HL-7702 cells models with low ASPP2 expression, respectively. Then, hepatocellular injury was induced by ethanol stimulation in vitro. Under ethanol stimulation, compared with that of the controls, the expression of PPARγ, phospho-mTOR, phospho-P70 S6 kinase, and phospho-S6 ribosomal protein of primary hepatocyte-ASPP2 siRNA and HL-7702-ASPP2 shRNA was significantly decreased (Fig. 2 E, F; Figure S1 A, B). In addition, ASPP2 adenovirus (Ad-ASPP2) was utilized to prepare the primary hepatocyte-Ad-ASPP2 and HL-7702-Ad-ASPP2 models. Western blotting analysis revealed that the overexpression of ASPP2 significantly increased the expression of PPARγ, phospho-mTOR, phospho-P70 S6 kinase, and phospho-S6 ribosomal protein (Fig. 2 G, H; Figure S1 C, D). Importantly, the expression of these proteins were the most significant changes when ethanol stimulation for 24 h in vitro.

Thus, these data suggest that ASPP2 promotes the activation of the PPARγ and mTOR signaling pathways in alcoholic liver injury.

ASPP2 deficiency reduces lipid accumulation in alcoholic liver injury by promoting fatty acid oxidation and transport and by inhibiting fatty acid synthesis and uptake

The pathway of fatty acid metabolism in the liver mainly includes fatty acid oxidation and transport, as well as fatty acid synthesis and uptake((Alves-Bezerra and Cohen 2017)). First, we examined the mRNA levels of genes involved in lipid metabolism in vivo. As shown in Fig. 3, we observed that the mRNA levels of VLDL secretion (*Apob, Mttp, Lfabp*) (Fig. 3A) and fatty acid oxidation (*Cpt1a, Aox*)-related genes (Fig. 3C) were decreased, whereas the mRNA levels of fatty acid uptake (*Cd36*) (Fig. 3B) and lipogenesis (*Acc1, Fas*)-related genes (Fig. 3D) were increased in ethanol-fed mice compared with pair-fed controls. Furthermore, ASPP2 deficiency regulated lipid metabolism by rescuing ethanol-mediated reductions in the mRNA levels of *Apob, Mttp, Lfabp*, *Cpt1a,* and *Aox* and the elevations in the mRNA levels of *Cd36*, *Acc1, and Fas* in ethanol-fed mice (Figs. 3 A-D).

Building upon the above findings for the mouse ALD model, we further examined the role of ASPP2 in the lipid metabolism of hepatocytes in vitro. Consistent with the above results in vivo, we demonstrated that the lower expression of ASPP2 significantly increased mRNA levels of *Apob, Mttp, Lfabp*, *Cpt1a,* and *Aox*; and significantly reduced mRNA levels of *Cd36*, *Acc1, and Fas* upon ethanol treatment compared to their corresponding controls (Figs. 3 E–H; Figure S2 A-D). Similarly, primary hepatocyte-ASPP2 siRNA and HL-7702-ASPP2 shRNA cell supernatant showed significantly higher ALT and AST activities and TC and TG levels than those of the control cell supernatant upon ethanol stimulation (Figs. 3 I, J; Figure S2 E, F). Simultaneously, the results showed that in ethanol-treated primary hepatocyte-Ad-ASPP2 and HL-7702-Ad-ASPP2 cells, the mRNA levels of *Apob, Mttp, Lfabp*, *Cpt1a,* and *Aox* were decreased, and the mRNA levels of *Cd36*, *Acc1, and Fas* were increased (Figures S3 A-D; Figure S3 G-J). Moreover, we found that compared with control, the levels of ALT, AST, TC, and TG were higher in the primary hepatocyte-Ad-ASPP2 and HL-7702-Ad-ASPP2 cell supernatant under ethanol stimulation (Figures S3E, F; Figure S3 K, L). Consistently, the differences in lipid metabolism-related gene expression and hepatocyte injury were most significant when alcohol was used for 24 h in vitro. Therefore, we selected 24 h as the ethanol intervention time point for the mechanistic study.

Therefore, these findings indicated that ASPP2 can aggravate ethanol-induced lipid accumulation by inhibiting fatty acid oxidation and VLDL secretion in hepatocytes and by promoting fatty acid synthesis and uptake.

ASPP2 deficiency improves ethanol-induced lipid accumulation via the PPARγ pathway in alcoholic liver injury

Our above data indicated that the PPARγ/mTOR signaling pathway may be involved in ASPP2-mediated lipid accumulation in alcoholic liver injury.

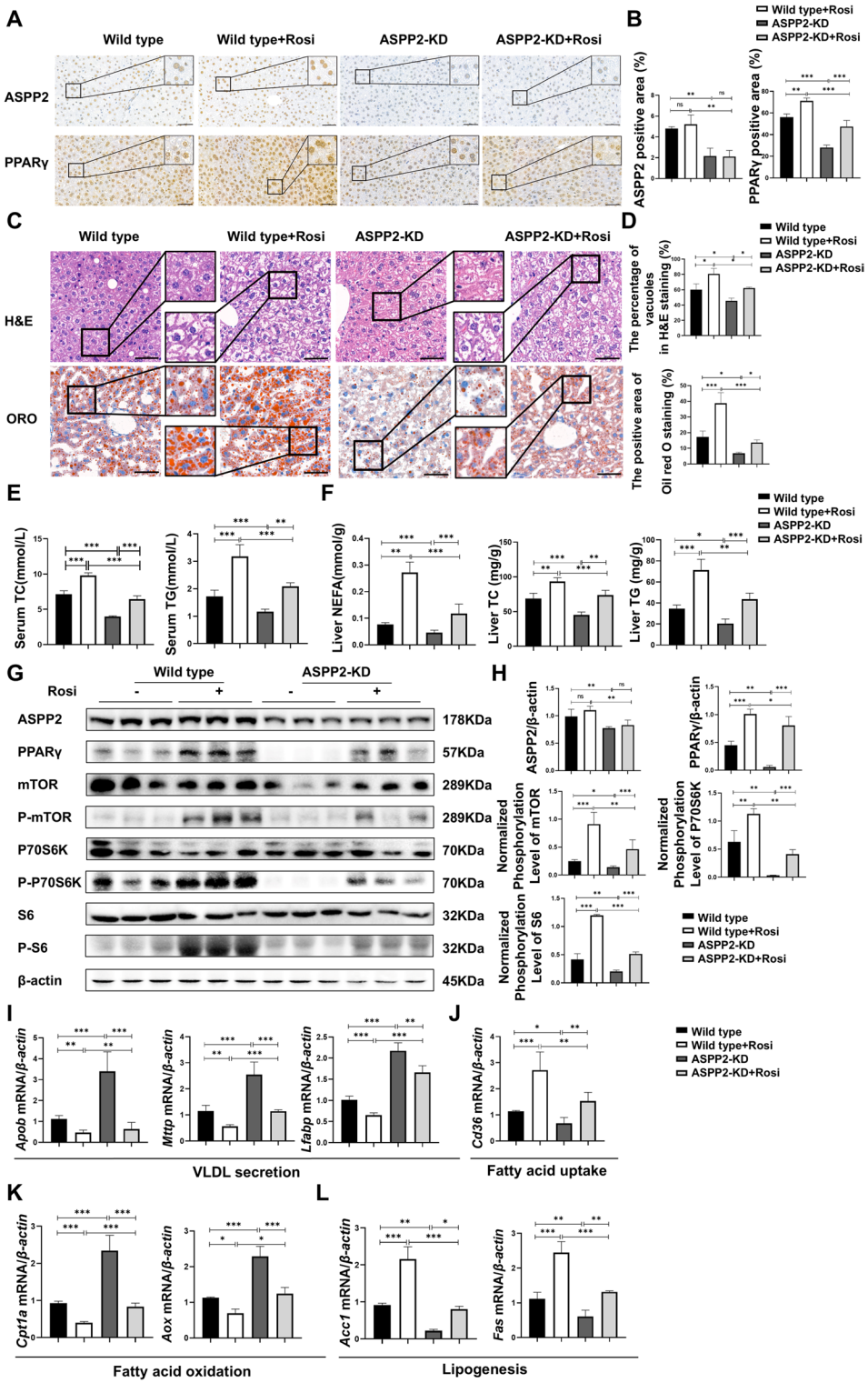
A
Wild type
Wild type+Rosi
ASPP2-KD
ASPP2-KD+Rosi
ASPP2
PPARγ
B
Wild type+Rosi
ASPP2-KD
ASPP2-KD+Rosi
ASPP2 positive area (%)
PPARγ positive area (%)
C
Wild type
Wild type+Rosi
ASPP2-KD
ASPP2-KD+Rosi
H&E
ORO
D
Wild type
Wild type+Rosi
ASPP2-KD
ASPP2-KD+Rosi
The percentage of vacuoles in H&E staining (%)
The positive area of Oil red O staining (%)
E
Wild type
Wild type+Rosi
ASPP2-KD
ASPP2-KD+Rosi
Serum TC(mmol/L)
Serum TG(mmol/L)
F
Liver NEFA(mmol/g)
Liver TC (mg/g)
Liver TG (mg/g)
G
Wild type
ASPP2-KD
Rosi
- + - +
ASPP2 178KDa
PPARγ 57KDa
mTOR 289KDa
P-mTOR 289KDa
P70S6K 70KDa
P-P70S6K 70KDa
S6 32KDa
P-S6 32KDa
β-actin 45KDa
H
ASPP2/β-actin
PPARγ/β-actin
Normalized Phosphorylation Level of mTOR
Normalized Phosphorylation Level of P70S6K
Normalized Phosphorylation Level of S6
Wild type
Wild type+Rosi
ASPP2-KD
ASPP2-KD+Rosi
I
Apob mRNA/β-actin
Mttp mRNA/β-actin
Lfabp mRNA/β-actin
VLDL secretion
J
Cd36 mRNA/β-actin
Fatty acid uptake
Wild type
Wild type+Rosi
ASPP2-KD
ASPP2-KD+Rosi
K
Cpt1a mRNA/β-actin
Aox mRNA/β-actin
Fatty acid oxidation
L
Acc1 mRNA/β-actin
Fas mRNA/β-actin
Lipogenesis

◂**Fig. 4** ASPP2 inhibits lipid metabolism through the PPARγ-mTOR signaling pathway in alcohol-induced mice models. (**A** and **B**) Representative IHC analysis of ASPP2 (top) and PPARγ (bottom) in liver sections, scar bar = 50 μm (**A**) and quantification analyses (B) of ASPP2 and PPARγ positive area (%) in mouse liver tissue from wild-type mice and ASPP2-KD mice with or without rosiglitazone (Rosi). The extended part of the black lines shows the enlarged image from the black box area. (**C**) Representative H&E staining (top) and Oil red O staining (bottom) of liver tissue, scar bar = 50 μm. (**D**) Analyses of the percentage of vacuoles in H&E staining (top) and the positive area in oil red O staining (bottom). (**E**) Serum TC and TG levels. (**F**) Liver NEFA, TC and TG levels. (**G** and **H**) western blot (**G**) and quantification analyses (**H**) of ASPP2, PPARγ, phospho-mTOR, phospho-S6, phospho-p70S6K, and β-actin in mouse liver tissue from wild-type mice and ASPP2-KD mice with or without Rosi. (**I**, **J**, **K**, and **L**) The mRNA levels of genes involved in lipid metabolism in mouse liver tissue from wild-type mice and ASPP2-KD mice with or without Rosi measured by real-time PCR. The values represent the means ± SEMs ($n = 6$ in each group). nsP > 0.05, $^{*}P < 0.05$, $^{**}P < 0.01$, $^{***}P < 0.001$. Independent-samples T tests between two groups and one-way ANOVA followed by Bonferroni post hoc test for multiple comparisons were used for statistical analyses

Wild-type mice and ASPP2-KD mice that received the ethanol diet were given the rosiglitazone (Rosi, PPARγ agonists) (5 mg/kg/Day) to explore the mechanism of ASPP2 regulating lipid metabolism via the PPARγ pathway in alcoholic liver injury. By immunohistochemistry analysis, we found that Rosi could promote the expression of PPARγ in mouse liver, but had no effect on the expression of ASPP2 (Fig. 4 A, B). This was consistent with the results of the protein expression level of ASPP2 in western blot (Fig. 4 G, H). In addition, the results in H&E staining and oil red O staining showed that Rosi increased the number and volume of vacuoles and lipid droplets in the liver of wild-type mice and ASPP2-KD mice, indicating that Rosi aggravated alcohol-induced steatosis and liver injury in both wild-type and ASPP2-KD mice. (Fig. 4 C, D). Moreover, Rosi increased the level of TC and TG in serum, and the level of NEFA, TC and TG in liver (Fig. 4 E, F). Next, by western blotting, we found that Rosi can promote the protein expression levels of phospho-mTOR, phospho-P70 S6 kinase, and phospho-S6 ribosomal protein (Fig. 4 G, H). And results showed that, the mRNA level of *Apob, Mttp, Lfabp*, *Cpt1a,* and *Aox* in mice treated with Rosi were lower than mice not treated with Rosi; the mRNA level of *Cd36*, *Acc1, and Fas* were higher in mice treated with Rosi (Fig. 4 I-L).

For further verification, primary hepatocytes/HL-7702 cells with low expression of ASPP2 upon ethanol stimulation were pretreated with Rosi. Immunofluorescence staining showed that the intensity of PPARγ-positive vesicles was much lower in HL-7702-ASPP2 shRNA cells than in Control, and Rosi significantly increased the expression of PPARγ (Figure S4 A, B). Consistently, the protein expression levels of PPARγ, phospho-mTOR, phospho-P70 S6 kinase, and phospho-S6 ribosomal protein exhibited the most dramatic increase after Rosi treatment, which offset the inhibitory effect of low ASPP2 expression. However, the expression of ASPP2 was not affected by Rosi (Figure S4 C, D). The same was true for primary hepatocytes with low ASPP2 expression (Fig. 5 A, B). Therefore, we further established that ASPP2 can regulate the expression of PPARγ-mTOR. Next, we examined the mRNA expression of genes related to lipid metabolism in HL-7702-ASPP2 shRNA and primary hepatocyte- ASPP2 siRNA, and we found that Rosi reversed the promotion of ASPP2 deletion on *Apob, Mttp, Lfabp*, *Cpt1a,* and *Aox* and the inhibition of *Cd36*, *Acc1, and Fas* (Figure S4 E–H; Fig. 5 C-F). Logically, the levels of ALT, AST, TC, and TG in the supernatant of cells decreased in cells with low expression of ASPP2, and Rosi treatment reversed the suppressive effect of ASPP2 downregulation on lipid accumulation and liver injury (Fig. S4 I, J; Fig. 5 G, H). In addition, Oil Red O staining showed that downregulation of ASPP2 reduced ethanol-induced accumulation of lipid droplets in HL-7702 cells, while pretreatment with Rosi reversed the inhibitory effect of ASPP2 downregulation on lipid droplets (Figure S4 K, L).

To make the experimental results more convincing, primary hepatocytes/HL-7702-Ad-ASPP2 cells were pretreated with the PPARγ inhibitor T0070907 for 2 h and then stimulated with ethanol for 24 h. Immunofluorescence results showed that T0070907 treatment reduced the expression of PPARγ in HL-7702-Ad-ASPP2 cells (Figures S5 A, B). At the protein level, in addition to inhibiting PPARγ, T0070907 also inhibited the expression of phospho-mTOR, phospho-P70 S6 kinase, and phospho-S6 ribosomal protein, while the expression of ASPP2 was not affected by T0070907 (Figure S5 C, D). This was also confirmed in ASPP2-overexpressing primary hepatocytes (Fig. 6 A, B). Further examination of the mRNA levels in lipid metabolism-related genes

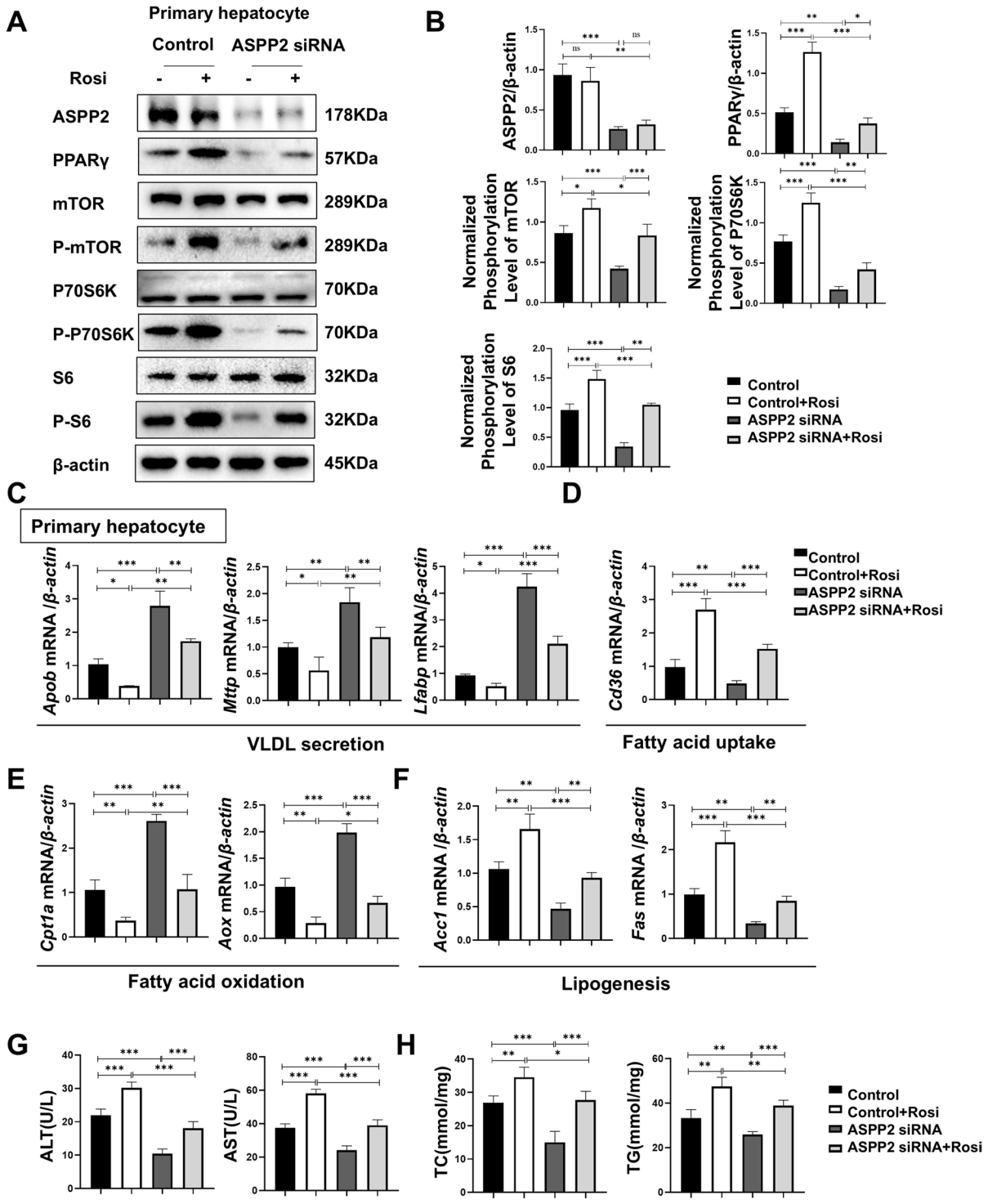
A
Primary hepatocyte
Control
ASPP2 siRNA
Rosi
ASPP2
PPARγ
mTOR
P-mTOR
P70S6K
P-P70S6K
S6
P-S6
β-actin
178KDa
57KDa
289KDa
289KDa
70KDa
70KDa
32KDa
32KDa
45KDa
B
ASPP2/β-actin
PPARγ/β-actin
Normalized Phosphorylation Level of mTOR
Normalized Phosphorylation Level of P70S6K
Normalized Phosphorylation Level of S6
Control
Control+Rosi
ASPP2 siRNA
ASPP2 siRNA+Rosi
C
Primary hepatocyte
Apob mRNA /β-actin
Mttp mRNA/β-actin
Lfabp mRNA/β-actin
VLDL secretion
D
Cd36 mRNA/β-actin
Fatty acid uptake
E
Cpt1a mRNA/β-actin
Aox mRNA/β-actin
Fatty acid oxidation
F
Acc1 mRNA /β-actin
Fas mRNA /β-actin
Lipogenesis
G
ALT(U/L)
AST(U/L)
H
TC(mmol/mg)
TG(mmol/mg)

◂**Fig. 5** ASPP2 inhibits lipid metabolism through the PPARγ-mTOR signaling pathway in alcohol-induced hepatocyte injury. (**A** and **B**) Western blot (**A**) and quantification analyses (**B**) of ASPP2, PPARγ, phospho-mTOR, phospho-S6, phospho-p70S6K, and β-actin in primary hepatocytes (Control and ASPP2 siRNA) with the indicated treatment. (**C**, **D**, **E**, and **F**) The mRNA levels of genes involved in lipid metabolism in primary hepatocytes (Control and ASPP2 siRNA) with the indicated treatment measured by real-time PCR. (**G**) ALT and AST levels in primary hepatocytes cell supernatant (Control and ASPP2 siRNA) with the indicated treatment. (**H**) TC and TG levels in primary hepatocytes cell supernatant (Control and ASPP2 siRNA) with the indicated treatment. nsP > 0.05, $^{*}P < 0.05$, $^{**}P < 0.01$, $^{***}P < 0.001$. The values represent the means ± SEMs ($n = 6$ in each group). Independent-samples T tests between two groups were used for statistical analysis, and one-way ANOVA followed by Bonferroni post hoc tests for multiple comparisons were used for statistical analyses

showed that T0070907 reversed ASPP2-induced hepatocyte lipid accumulation by promoting *Apob, Mttp, Lfabp*, *Cpt1a,* and *Aox* and inhibiting *Cd36*, *Acc1, and Fas* (Figure S5 E–H; Fig. 6 C-F). We also found that T0070907 could effectively counteract the promoting effect of adenovirus-mediated overexpression of ASPP2 on ALT, AST, TC, and TG, further ameliorating the suppressive effect of ASPP2 upregulation on lipid metabolism in HL-7702 cells and primary hepatocytes (Figures S5 I, J; Fig. 6 G, H). Furthermore, by oil Red O staining, we found that elevated ASPP2 further aggravated ethanol-induced lipid droplet accumulation in HL-7702 cells, while T0070907 pretreatment alleviated the effect of elevated ASPP2 on lipid droplet accumulation (Figure S5 K, L).

These results provide compelling evidence that ASPP2 deficiency decreases ethanol-induced lipid metabolism disorder and hepatic steatosis through the PPARγ-mTOR pathway.

ASPP2 induces lipid accumulation in ALD patients through the PPARγ-mTOR signaling pathway

Finally, we validated our results in patients with alcoholic cirrhosis. First, the expression of ASPP2 and PPARγ in patients with an alcoholic liver was detected by immunohistochemistry, and the results showed that ASPP2 and PPARγ were significantly increased in liver tissues of patients with alcoholic liver cirrhosis compared with normal controls. ASPP2 was mainly expressed in the nucleus, while PPARγ was expressed in the nucleus and cytoplasm (Fig. 7 A, B). We verified the mRNA expression levels of *Aspp2* and *Pparγ*, and found that the expressions of both were increased in the liver tissues of patients with ALD (Fig. 7 C). In addition, H&E staining showed marked steatosis in ALD patients (Fig. 7 D). At the same time, western blot results showed that the expression levels of ASPP2, PPARγ, phospho-mTOR, phospho-P70 S6 kinase and phospho-S6 ribosomal protein were increased in the liver tissues of ALD patients (Fig. 7 E, F). In addition, patients with ALD also showed significant abnormalities in lipid metabolism, with decreased mRNA levels of *Apob, Mttp, Lfabp*, *Cpt1a,* and *Aox* and increased mRNA levels of *Cd36*, *Acc1, and Fas* (Figure S6 A-D).

Overall, these results confirmed that ASPP2 may induce lipid accumulation in patients with ALD through the PPARγ/mTOR signaling pathway.

Discussion

In this study, we found that ASPP2 can induce lipid accumulation through the PPARγ signaling pathway in ALD, and ASPP2 regulates lipid metabolism by promoting fatty acid synthesis and uptake and inhibiting fatty acid oxidation and VLDL secretion. Mechanically, we speculated that ASPP2 localized in the nucleus was activated under the induction of alcohol, which further promoted the expression of PPARγ. PPARγ entered the cytoplasm, and the increased expression of PPARγ further induced the activation of the mTOR signaling pathway, thereby triggering lipid accumulation.

The most important finding of this study is that ASPP2 can promote ethanol-induced lipid accumulation. In this study, we found that reduction of hepatic ASPP2 effectively alleviated lipid accumulation in the liver of ethanol-fed wild-type mice. In vivo and in vitro, we further confirmed that ASPP2 induced hepatic lipid accumulation in alcoholic liver injury by promoting fatty acid uptake and synthesis and inhibiting fatty acid oxidation and VLDL secretion. Consistent with the findings in our research, Che Yang et al. identified that ASPP2 can promote lipid accumulation in the liver and exacerbate hepatic steatosis (Che 2022). In addition, results from another research suggested that ASPP2 knockdown mitigated hepatocyte damage and steatosis in HBV-infected mice (Wang et al. 2022a). And our previous studies have

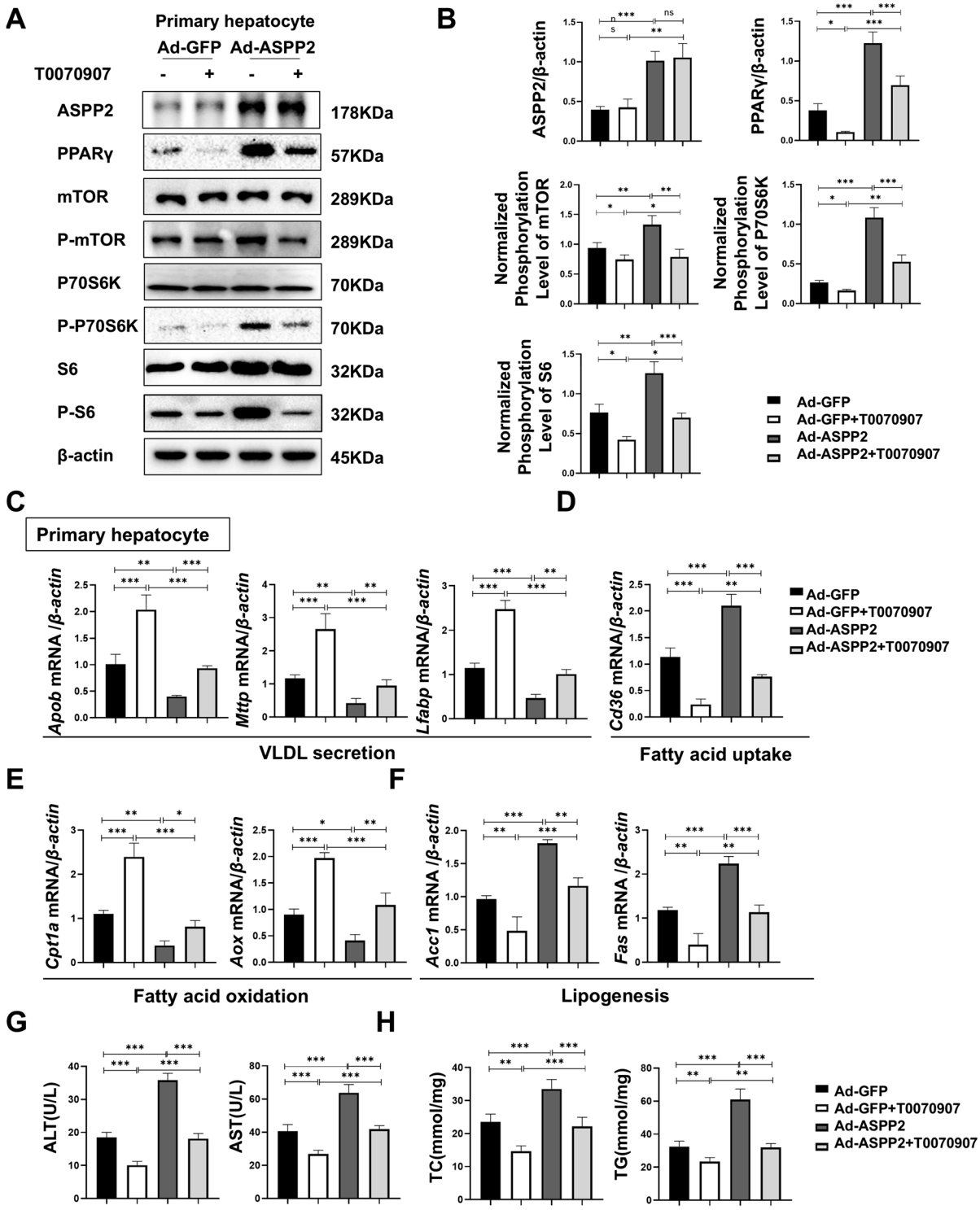
A
Primary hepatocyte
Ad-GFP Ad-ASPP2
T0070907 - + - +
ASPP2 178KDa
PPARγ 57KDa
mTOR 289KDa
P-mTOR 289KDa
P70S6K 70KDa
P-P70S6K 70KDa
S6 32KDa
P-S6 32KDa
β-actin 45KDa
B
ASPP2/β-actin
PPARγ/β-actin
Normalized Phosphorylation Level of mTOR
Normalized Phosphorylation Level of P70S6K
Normalized Phosphorylation Level of S6
Ad-GFP
Ad-GFP+T0070907
Ad-ASPP2
Ad-ASPP2+T0070907
C
Primary hepatocyte
Apob mRNA /β-actin
Mttp mRNA/β-actin
Lfabp mRNA/β-actin
Cd36 mRNA/β-actin
VLDL secretion
Fatty acid uptake
D
E
Cpt1a mRNA/β-actin
Aox mRNA/β-actin
Fatty acid oxidation
F
Acc1 mRNA /β-actin
Fas mRNA /β-actin
Lipogenesis
G
ALT(U/L)
AST(U/L)
H
TC(mmol/mg)
TG(mmol/mg)

◂**Fig. 6** ASPP2 inhibits lipid metabolism through the PPARγ-mTOR signaling pathway in alcohol-induced hepatocyte injury. (**A** and **B**) Western blot (**A**) and quantification analyses (**B**) of ASPP2, PPARγ, phospho-mTOR, phospho-S6, phospho-p70S6K, and β-actin in primary hepatocytes (Ad-GFP and Ad-ASPP2) with the indicated treatment. (**C**, **D**, **E**, and **F**) The mRNA levels of genes involved in lipid metabolism in primary hepatocytes (Ad-GFP and Ad-ASPP2) with the indicated treatment measured by real-time PCR. (**G**) ALT and AST levels in primary hepatocytes cell supernatant (Ad-GFP and Ad-ASPP2) with the indicated treatment. (**H**) TC and TG levels in primary hepatocytes supernatant (Ad-GFP and Ad-ASPP2) with the indicated treatment. The values represent the means ± SEMs ($n=6$ in each group). nsP > 0.05, *$P<0.05$, **$P<0.01$, ***$P<0.001$. Independent-samples T tests between two groups were used for statistical analysis, and one-way ANOVA followed by Bonferroni post hoc tests for multiple comparisons were used for statistical analyses

also suggested that ASPP2 deficiency has a protective effect against liver damage (Xu et al. 2019). Still, there were two researches contradict our study. The first one suggested that ASPP2 may reduce the level of triglycerides by inhibiting autophagy in NAFLD, but its regulatory mechanism for lipid metabolism was not specifically elucidated (Xie et al. 2015). And the second paper suggested lipid accumulation in ASPP2$^{\pm}$ mice induced by MCD diet involves to other factors such as gut microbiota (Xie et al. 2022). We speculate that these different but interesting findings may be due to the difference in alcohol and lipid metabolic pathways. In addition to the lipid metabolic function of the liver, the lipid accumulation induced by NAFLD also involves other factors such as intestinal function. But about 95% of alcohol is metabolized directly in the liver, so the mechanism of lipid metabolism dysregulation induced by NAFLD may be different from that induced by alcohol, which deserves further exploration [(Toshikuni et al. 2014); (2022)].

The second major finding was that ASPP2 exacerbates lipid metabolism in ALD through PPARγ signaling. PPARγ is an important regulator in the lipid metabolism pathway (Xiong et al. 2022), which plays a crucial role in the development of steatosis by increasing the expression of proteins related to fatty acid uptake (Silva and Peixoto 2018), activating the de novo synthesis of fatty acids (Piccinin et al. 2019) and promoting the formation and storage of triglycerides in lipid droplets (Montaigne et al. 2021). PPARγ is considered to be an endonuclear receptor (Chandra et al. 2008), and its enhanced activity is manifested by a significant increase in binding to DNA in vivo, leading to increased expression of its downstream target genes that are involved in lipid metabolism processes (Choi et al. 2021). It was reported that ethanol exposure downregulated adipose PPARγ gene and reduced the white adipose tissue mass in association with induction of inflammation, which was attenuated by rosiglitazone (Sun et al. 2012). PPARγ activation in vivo reduced alcohol-mediated impairments in lung bacterial clearance (Yeligar et al. 2016). In addition, adipose-derived mesenchymal stem cells can regulate lipid metabolism and lipid droplet biogenesis in macrophages through PPARγ signaling (Souza-Moreira et al. 2019). Several reports have recently indicated that in NAFLD patients, a significant increase in PPARγ expression levels in the liver leads to an increase in the expression of downstream lipogenic genes and induce hepatic steatosis [(Skat-Rørdam et al. 2019); (Li et al. 2020)]. Therefore, the role of PPARγ in different organs is not consistent and PPARγ may play organ-specific role in liver disease. Unfortunately, in this study, the mechanism by which ASPP2 regulates PPARγ remains unclear, and it may be related to the transcriptional activity of PPARγ. But we found that ASPP2 may directly bind and interact with PPARγ using the researcher platform for protein–protein molecular docking tools (https://www.home-for-researchers.com/static/index.html#/). We select the three-dimensional structure of ASPP2 and PPARγ proteins from the PDB database, and got the molecular docking diagram (Figure S7). And the two amino acids connected by the red dashed lines represent the forcingsites of ASPP2 and PPARγ. The mutual combination between ASPP2 and PPARγ still needs further experimental verification.

As the theoretical basis of this study, previous findings reviewed that PPARγ is strongly induced in NAFLD, and increased expression of PPARγ in the liver promotes steatosis (2021); (2023). What's more, similar to our study, Zhang et al. showed PPARγ contributes to alcohol-induced hepatic steatosis (Zhang et al. 2016). Some studies have shown that mTOR plays an important role in lipid metabolism and PPARγ may regulate lipometabolism through mTOR signaling pathway [(Wang et al. 2015); (Mossmann et al. 2018); (Laplante and Sabatini 2009)]. Xiangyu Hu's study suggested that the PPAR-γ/mTOR signaling pathway was involved in the lipid metabolism of NK cells in mice with high plasma triglycerides. The expression of PPARγ is increased in the cytoplasm,

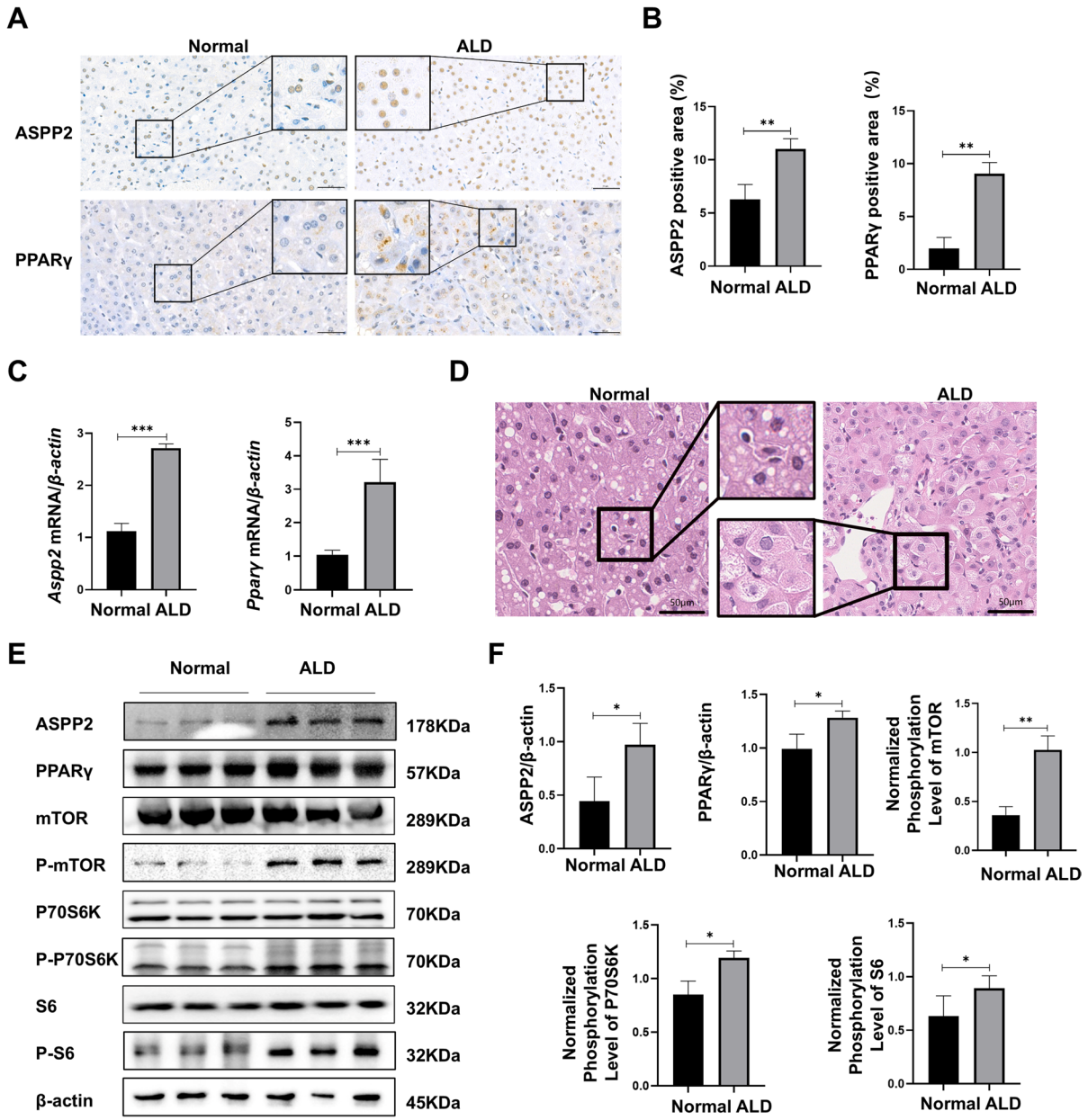

Fig. 7 ASPP2 induces hepatocyte lipid accumulation in ALD patients through the PPARγ-mTOR signaling pathway. The patients with ALD were enrolled from inpatients in Beijing Youan Hospital, Capital Medical University. The diagnosis of ALD was based on guidelines for the prevention and treatment of ALD (2018 version). (A and B) Representative IHC analysis of ASPP2 and PPARγ in liver sections, scar bar = 50 μm (**A**) and quantification analyses (**B**) of ASPP2- and PPARγ-positive areas (%). (**C**) The mRNA expression levels of Aspp2 and Pparγ measured by real-time PCR. (**D**) Representative photomicrographs of H&E-stained liver sections, scar bar = 50 μm. (**E** and **F**) western blot (**E**) and quantification analyses (**F**) of ASPP2, PPARγ, phospho-mTOR, phospho-S6, phospho-p70S6K, and β-actin in ALD patients. The values represent the means ± SEMs ($n = 4$ in each group). nsP > 0.05, $^{*}P < 0.05$, $^{**}P < 0.01$, $^{***}P < 0.001$. Independent-samples T tests between two groups were used for statistical analysis, and one-way ANOVA followed by Bonferroni post hoc tests for multiple comparisons were used for statistical analyses

which further regulates the activity of its downstream mTOR signaling pathway. In addition, PPARγ can enhance the expression of PTEN, which regulates the pathway of PI3K-AKT-mTORC1, eventually led to lipid accumulation (Hu et al. 2021). Other studies reported that activation of the mTOR/PPARγ pathway can induce an increase in triglyceride content and lead to abnormal lipid metabolism (Zhu et al. 2021).

Given the association of the ASPP2, PPARγ, and mTOR signaling pathways, we explored the mechanism that ASPP2 regulates lipid metabolism in ALD. The expression of ASPP2 and PPARγ was increased in ethanol-fed mice and ALD patients. In addition, knockdown of ASPP2 significantly decreased PPARγ expression and mTOR phosphorylation in ethanol-induced HL-7702 cells and primary hepatocyte, whereas the opposite results were obtained by overexpression of ASPP2. Furthermore, the reduction of hepatic ASPP2 reduced hepatic PPARγ and P-mTOR expression and alleviated lipid accumulation in ethanol-fed mice. More importantly, the PPARγ agonist could counteract the protective effect of ASPP2 knockdown on ethanol-induced lipid accumulation and promote the phosphorylation of mTOR and downstream molecules. On the contrary, the PPARγ inhibitor reversed the promotive effect of ASPP2 overexpression on lipid accumulation. Therefore, ASPP2 could regulate lipid metabolism through PPARγ-mTOR signaling pathway in ALD.

The steatosis of ALD is mainly manifested by increased fatty acid synthesis and uptake, decreased fatty acid oxidation and VLDL secretion (You and Arteel 2019). A study found that ethanol can promote fatty acid synthesis, which is characterized by significant upregulation of the protein expression of ACC and FAS (Bian et al. 2021). Simultaneously, ethanol also reduced the protein level of CPT1A, a key enzyme of fatty acid β-oxidation (2022). Some studies have also found that ethanol can promote the uptake of fatty acids in hepatocytes (Wang et al. 2022b). Consistent with the above studies, we also found that ethanol could promote fatty acid synthesis (ACC1, FAS) and uptake (CD36) in hepatocytes and inhibit VLDL secretion (apoB, MTTP, LFABP) and fatty acid oxidation (CPT1A, AOX).

Although this study verified that ASPP2 can regulate the PPARγ-mTOR signaling pathway, the molecular mechanism by which ASPP2 is increased in ALD needs to be further studied. In other words, whether the elevation of ASPP2 is caused directly by alcohol and its derivatives or through other molecular-mediated interactions remains unclear, which need further to explore in our follow-up study. In addition, despite there is a tremendous amount of data with multiple effects on both hepatic steatosis and injury described along with changes in almost every step of lipid metabolism, in the end, what is the primary effect of ASPP2 and what are secondary effects are unclear.

Conclusion

In this study, we determined that ASPP2 exacerbates ethanol-induced hepatic injury and lipid metabolism disorder by upregulating the PPARγ signaling pathway. Therefore, ASPP2 may be a new target for treating ALD in the future.

Acknowledgements Not applicable.

Author contributions Y. Z. performed the experiments, analyzed the data and wrote the manuscript; XZ. M., F. L. and HL. S. assisted with generation of ALD mouse models and contributed to tissue samples collection; DX. C. provided the ASPP2 knockdown mice; Y.C., YM. M. and HB. S. conceived the study, designed the experiments, and revised the manuscript.

Funding This work was supported by National Key Research and Development Program of China (2022YFC2305002); Beijing Nova Program (20220484201); Beijing Hospitals Authority's Ascent Plan (DFL20221501); Construction Project of High-level Technology Talents in Public Health (Discipline leader -01–12).

Data availability No datasets were generated or analysed during the current study.

Declarations

Ethics approval and consent to participate The study using human tissue samples was approved by the Ethics Committee of Beijing You'an Hospital, Capital Medical University, China (Jingyoukelun2022037) and was conducted in accordance with the Declaration of Helsinki. Animal experiments were approved by the Animal Experiments and Experimental Animal Welfare Committee of Capital Medical University (AEEI-2022–117) and were performed in accordance with the Basel Declaration.

Consent for publication Not applicable.

Conflict of interests The authors declare no competing interests.

References

Alves-Bezerra M, Cohen DE. Triglyceride Metabolism in the Liver. Compr Physiol. 2017;8(1):1–8.

Bajaj JS. Alcohol, liver disease and the gut microbiota. Nat Rev Gastroenterol Hepatol. 2019;16(4):235–46.

Bertola A, et al. Mouse model of chronic and binge ethanol feeding (the NIAAA model). Nat Protoc. 2013;8(3):627–37.

Bian L, et al. Mori Fructus Polysaccharides Attenuate Alcohol-Induced Liver Damage by Regulating Fatty Acid Synthesis, Degradation and Glycerophospholipid Metabolism in Mice. Front Pharmacol. 2021;12: 766737.

Chandra V, et al. Structure of the intact PPAR-gamma-RXR- nuclear receptor complex on DNA. Nature. 2008;456(7220):350–6.

Che Y. Experimental study of molecular mechanism of ASPP2 promoting lipid accumulation in hepatocytes. Beijing Med J. 2022;44(1):49–53.

Choi Y, et al. Liver-Specific Deletion of Mouse CTCF Leads to Hepatic Steatosis via Augmented PPARγ Signaling. Cell Mol Gastroenterol Hepatol. 2021;12(5):1761–87.

Fuster D, Samet JH. Alcohol Use in Patients with Chronic Liver Disease. N Engl J Med. 2018;379(13):1251–61.

Hu X, et al. Downregulation of NK cell activities in Apolipoprotein C-III-induced hyperlipidemia resulting from lipid-induced metabolic reprogramming and crosstalk with lipid-laden dendritic cells. Metabolism. 2021;120: 154800.

Laplante M, Sabatini DM. An emerging role of mTOR in lipid biosynthesis. Curr Biol. 2009;19(22):R1046–52.

Lee SM, Muratalla J, Sierra-Cruz M, Cordoba-Chacon J. Role of hepatic peroxisome proliferatoractivated receptor γ in non-alcoholic fatty liver disease. J Endocrinol. 2023;257(1):e220155. https://doi.org/10.1530/JOE-22-0155.

Li DM, Wu YX, Hu ZQ, Wang TC, Zhang LL, Zhou Y, et al. Lactoferrin prevents chronic alcoholic injury by regulating redox balance and lipid metabolism in female C57BL/6J mice. Antioxidants (Basel). 2022;11(8):1508. https://doi.org/10.3390/antiox11081508.

Li L, et al. Hepatocyte-specific Nrf2 deficiency mitigates high-fat diet-induced hepatic steatosis: Involvement of reduced PPARγ expression. Redox Biol. 2020;30: 101412.

Malnick SDH, Alin P, Somin M, Neuman MG. Fatty liver disease-alcoholic and non-alcoholic: similar but different. Int J Mol Sci. 2022;23(24):16226. https://doi.org/10.3390/ijms232416226.

Monroy-Ramirez HC, Galicia-Moreno M, Sandoval-Rodriguez A, Meza-Rios A, Santos A, Armendariz-Borunda J. PPARs as metabolic sensors and therapeutic targets in liver diseases. Int J Mol Sci. 2021;22(15):8298. https://doi.org/10.3390/ijms22158298.

Montaigne D, Butruille L, Staels B. PPAR control of metabolism and cardiovascular functions. Nat Rev Cardiol. 2021;18(12):809–23.

Mossmann D, Park S, Hall MN. mTOR signalling and cellular metabolism are mutual determinants in cancer. Nat Rev Cancer. 2018;18(12):744–57.

Ouyang Q, Liu R. MTOR-mediates hepatic lipid metabolism through an autophagic SNARE complex. Autophagy. 2022;18(6):1467–9.

Piccinin E, Villani G, Moschetta A. Metabolic aspects in NAFLD, NASH and hepatocellular carcinoma: the role of PGC1 coactivators. Nat Rev Gastroenterol Hepatol. 2019;16(3):160–74.

Sehrawat TS, Liu M, Shah VH. The knowns and unknowns of treatment for alcoholic hepatitis. Lancet Gastroenterol Hepatol. 2020;5(5):494–506.

Silva AKS, Peixoto CA. Role of peroxisome proliferator-activated receptors in non-alcoholic fatty liver disease inflammation. Cell Mol Life Sci. 2018;75(16):2951–61.

Singal AK, et al. ACG Clinical Guideline: Alcoholic Liver Disease. Am J Gastroenterol. 2018;113(2):175–94.

Skat-Rørdam J, et al. A role of peroxisome proliferator-activated receptor γ in non-alcoholic fatty liver disease. Basic Clin Pharmacol Toxicol. 2019;124(5):528–37.

Song B, et al. Downregulation of ASPP2 in pancreatic cancer cells contributes to increased resistance to gemcitabine through autophagy activation. Mol Cancer. 2015;14:177.

Souza-Moreira L, et al. Adipose-derived Mesenchymal Stromal Cells Modulate Lipid Metabolism and Lipid Droplet Biogenesis via AKT/mTOR -PPARγ Signalling in Macrophages. Sci Rep. 2019;9(1):20304.

Sun X, et al. Activation of peroxisome proliferator-activated receptor-γ by rosiglitazone improves lipid homeostasis at the adipose tissue-liver axis in ethanol-fed mice. Am J Physiol Gastrointest Liver Physiol. 2012;302(5):G548–57.

Tian L, et al. Downregulation of ASPP2 promotes gallbladder cancer metastasis and macrophage recruitment via aPKC-ι/GLI1 pathway. Cell Death Dis. 2018;9(11):1115.

Toshikuni N, Tsutsumi M, Arisawa T. Clinical differences between alcoholic liver disease and nonalcoholic fatty liver disease. World J Gastroenterol. 2014;20(26):8393–406.

Turnquist C, et al. STAT1-induced ASPP2 transcription identifies a link between neuroinflammation, cell polarity, and tumor suppression. Proc Natl Acad Sci U S A. 2014;111(27):9834–9.

Wang Y, et al. Transcriptional regulation of hepatic lipogenesis. Nat Rev Mol Cell Biol. 2015;16(11):678–89.

Wang Y, et al. ASPP2 reduction attenuates HBV induced chronic liver damage: A hybrid mouse model study. Biochem Biophys Res Commun. 2022a;610:61–9.

Wang X, et al. Hepatoprotective effects of sea cucumber etherphospholipids against alcohol-induced lipid metabolic dysregulation and oxidative stress in mice. Food Funct. 2022b;13(5):2791–804.

Xie F, et al. ASPP2 attenuates triglycerides to protect against hepatocyte injury by reducing autophagy in a cell and mouse model of non-alcoholic fatty liver disease. J Cell Mol Med. 2015;19(1):155–64.

Xie F, et al. Dysregulated hepatic lipid metabolism and gut microbiota associated with early-stage NAFLD in ASPP2-deficiency mice. Front Immunol. 2022;13: 974872.

Xiong S, et al. Enhanced lipogenesis through Pparγ helps cavefish adapt to food scarcity. Curr Biol. 2022;32(10):2272-2280.e6.

Xu D, et al. A Hepatocyte-Mimicking Antidote for Alcohol Intoxication. Adv Mater. 2018;30(22): e1707443.

Xu P, et al. Deficiency of apoptosis-stimulating protein 2 of p53 protects mice from acute hepatic injury induced by CCl(4) via autophagy. Toxicol Lett. 2019;316:85–93.

Yao J, et al. ASPP2 Coordinates ERS-Mediated Autophagy and Apoptosis Through mTORC1 Pathway in Hepatocyte Injury Induced by TNF-α. Front Pharmacol. 2022;13: 865389.

Yeligar SM, et al. Peroxisome Proliferator-Activated Receptor γ Regulates Chronic Alcohol-Induced Alveolar Macrophage Dysfunction. Am J Respir Cell Mol Biol. 2016;55(1):35–46.

You M, Arteel GE. Effect of ethanol on lipid metabolism. J Hepatol. 2019;70(2):237–48.

Zhang W, et al. Hepatic Peroxisome Proliferator-Activated Receptor Gamma Signaling Contributes to Alcohol-Induced Hepatic Steatosis and Inflammation in Mice. Alcohol Clin Exp Res. 2016;40(5):988–99.

Zhu Y, et al. Decabromodiphenyl ether disturbs hepatic glycolipid metabolism by regulating the PI3K/AKT/GLUT4 and mTOR/PPARγ/RXRα pathway in mice and L02 cells. Sci Total Environ. 2021;763: 142936.